

## Role of Stress in Thin Film Alloy Thermodynamics: Competition between Alloying and Dislocation Formation

G. E. Thayer,<sup>2,1</sup> V. Ozolins,<sup>1</sup> A. K. Schmid,<sup>1</sup> N. C. Bartelt,<sup>1</sup> M. Asta,<sup>1</sup> J. J. Hoyt,<sup>1</sup> S. Chiang,<sup>2</sup> and R. Q. Hwang<sup>1</sup>

<sup>1</sup>*Sandia National Laboratories, Livermore, California 94551*

<sup>2</sup>*Department of Physics, University of California at Davis, Davis, California 95616*

(Received 22 September 2000)

Using scanning tunneling microscopy (STM) and first-principles local-spin-density-approximation calculations to study submonolayer films of  $\text{Co}_{1-c}\text{Ag}_c/\text{Ru}(0001)$  alloys, we have discovered a novel phase-separation mechanism. When the Ag concentration  $c$  exceeds 0.4, the surface phase separates between a dislocated, pure Ag phase and a pseudomorphically strained  $\text{Co}_{0.6}\text{Ag}_{0.4}$  surface alloy. We attribute the phase separation to the competition between two stress relief mechanisms: surface alloying and dislocation formation. The agreement between STM measurements and our calculated phase diagram supports this interpretation.

DOI: 10.1103/PhysRevLett.86.660

PACS numbers: 68.35.Md, 05.70.Np, 81.30.Bx

Since thermodynamic phase diagrams of bulk alloys are a starting point to understanding many important material properties, much effort has been devoted towards studying them. It has been found that phase diagrams are governed by a combination of chemical and size effects of the alloy constituents. For instance, the Hume-Rothery condition states that it is difficult to form solid solutions of metals whose atomic diameters differ by more than 15% [1]. Recently, the discovery of new thin film surface alloys has led to an investigation of additional effects intrinsic to surfaces, such as stress due to lattice mismatch between film and substrate. Since surface stress can be relieved in a variety of ways, there exist fundamentally different relationships between the size differences of alloy constituents and phase diagrams in surface alloys. The purpose of this Letter is to probe how the phase diagram of surface alloys depends on stress relaxation mechanisms.

Lattice mismatch between a film and a substrate introduces stress that can significantly influence film structure. For single component films, the buildup of strain energy with film thickness is relieved through the formation of dislocations at a critical thickness, which for metals is typically on the order of a few monolayers [2,3]. For multi-component films, however, alternative mechanisms for stress relief are possible, such as alloy formation [4]. This mechanism has been found to cause alloying of bulk immiscible metals in thin film configurations [4–7]. In the work presented here, we describe how the competition between these two stress relief mechanisms can affect the phase diagram of a thin film alloy. This is demonstrated by a study of the alloy structure of submonolayer Co-Ag films grown on the Ru(0001) surface. We have experimentally observed regions of the phase diagram where the structure of the film is dominated either by alloying or by dislocation formation, with an intermediate coexistence regime. These results are compared to first-principles calculations of the phase diagram to quantify the energetic balance between these two stress relief mechanisms as a function of composition.

The single component systems of Co/Ru(0001) and Ag/Ru(0001) have been studied by a variety of spectroscopic and topographic techniques, and it is known that single monolayer films of Ag on Ru contain a dislocation network [2], while a monolayer Co film does not [8]. Neither Co nor Ag is soluble with Ru [8–10] at temperatures and time scales relevant to our experiment. The mixture of Co-Ag on Ru(0001) is interesting because the atomic size of Ag is larger than Ru, while that of Co is smaller. This can lead to the formation of Co-Ag alloy films in the first monolayer over a wide range of compositions.

All of the experimental results reported here are from films that were deposited at room temperature, annealed to 500 °C, and then cooled to room temperature for imaging. At this annealing temperature, the mobility of the film components is sufficiently high that the imaged structure represents the equilibrium state at a temperature between room temperature and 500 °C. Although the total coverage of Co and Ag was less than 1 ML (monolayer) for every film we investigated, the structure of the phases we observed did not depend on total coverage, but only on the relative Co-Ag composition.

Co-rich submonolayer films exhibit an alloy structure similar to that of the  $\text{Co}_{0.75}\text{Ag}_{0.25}$  film shown in Fig. 1(a). This image shows an atomic step of Ru and two terraces. The black background in the image is the lower terrace of the Ru substrate. The Co-Ag alloy film is shown on this lower terrace, emerging from the step edge. Darker areas of the alloy film are pure Co, while the smaller, lighter-colored regions are Ag. The Ag in this alloy is not atomically dispersed, but rather forms small irregular droplets of approximately 15 atoms each. This general structure persists up to a composition of approximately  $\text{Co}_{0.6}\text{Ag}_{0.4}$ , with the size and density of the droplets increasing as the amount of Ag increases.

For compositions containing more than 40% Ag, the film is found to decompose in two distinct phases. This is shown in the image in Fig. 1(b) of a film composed of 20% Co and 80% Ag. The alloy phase of the film in Fig. 1(b) is

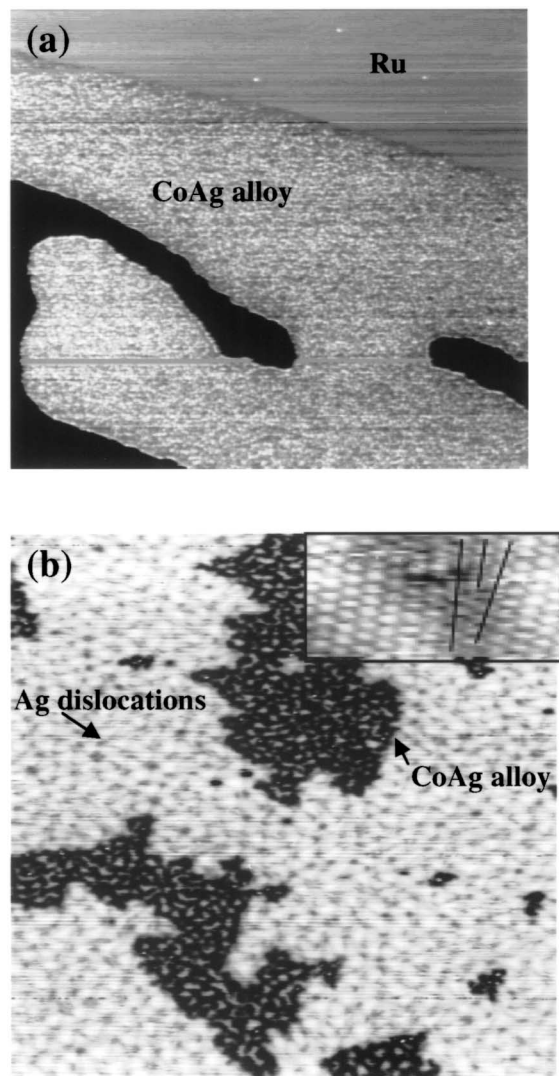


FIG. 1. Equilibrated Co-Ag films on Ru(0001). Phase segregation occurs for films with Ag composition greater than 40%. (a)  $1890 \text{ \AA} \times 1680 \text{ \AA}$  image ( $I_t = 0.24 \text{ nA}$ ,  $V_s = -0.16 \text{ V}$ ) of submonolayer alloy film with composition of 25% Ag shown against two Ru terraces in the background. (b)  $1000 \text{ \AA} \times 1000 \text{ \AA}$  image ( $I_t = 0.50 \text{ nA}$ ,  $V_s = 0.58 \text{ V}$ ) of film with composition of 80% Ag. Inset shows atomic resolution of a single dislocation in the pure Ag phase, showing a missing row of atoms in the atomic lattice.

similar to the disordered droplet structure of the alloy film shown in Fig. 1(a); however, the alloy phase in Fig. 1(b) is measured to have a composition of  $\text{Co}_{0.6}\text{Ag}_{0.4}$ . The Ag patches in this alloy phase ( $\sim 20$  atoms in size) are apparent. The alloy phase coexists with a pure Ag phase that has a misfit dislocation structure. This structure is similar to that found in the pure Ag/Ru(0001) system, which is composed of a  $(16 \times \sqrt{3})$  unit cell with 15 Ag atoms for every 16 Ru atoms [2,11]. The phase separation is found in all films with Ag concentration exceeding 40%, with the alloy phase maintaining the same  $\text{Co}_{0.6}\text{Ag}_{0.4}$  composition.

Atomically resolved STM images reveal the absence of dislocations in the alloy phase (Fig. 2). The Co atoms in Fig. 2 appear light and the Ag atoms are dark. Because of

imaging conditions, the contrast in this image is opposite to the contrast in Fig. 1. There are no displacements of atoms that indicate the presence of either threading dislocations or partial dislocations in the film plane. Note, however, that the Co atoms along the borders of Ag droplets are imaged substantially brighter than Co atoms located farther from these boundaries. A plausible interpretation is that these brighter boundary atoms are shifted due to a relaxation of the compressively stressed Ag droplets that causes these atoms to rise out of the hollow sites of the substrate. The contrast does of course include both topographic and electronic effects.

These results can be qualitatively explained in terms of a competition between two stress relief mechanisms, alloying and dislocation formation. The Co(111) lattice (nearest-neighbor distance of  $2.50 \text{ \AA}$ ) is smaller than the Ru(0001) ( $2.71 \text{ \AA}$ ) substrate by approximately 7%, while the Ag(111) lattice ( $2.89 \text{ \AA}$ ) is larger by about 8%. This mismatch between film and substrate is mediated by the mixing of Co and Ag and results in a structure of lower stress and higher commensurability with the substrate [4]. The alloy phase therefore has lower surface energy compared to pseudomorphic single component films, as found in the Co-rich portion of the phase diagram. On the other hand, since the bulk phase diagram of Co-Ag exhibits a large miscibility gap extending into the liquid state [12], we infer that alloying is energetically costly due to unfavorable Co-Ag bonds. Therefore as the concentration of Ag in the film increases, the total cost of extra Co-Ag bonds grows above that of the formation of a pure Ag phase with dislocations, leading to the observed coexistence region with the  $\text{Co}_{0.6}\text{Ag}_{0.4}$  alloy. This simple picture is also consistent with the alloy phase consisting of Ag “droplets” as opposed to an atomically dispersed alloy. The droplet size is determined by the competition between the relaxation energy of the droplet and the cost of forming Co-Ag bonds at the droplet perimeter [4,13,14].

To quantify this interpretation of our experimental results, we used first-principles local-spin-density-approximation (LSDA) calculations to calculate the  $T = 0 \text{ K}$  phase diagram of this system. These calculations predict that droplet and stripe configurations are energetically favored in Co-rich alloys and a two-phase region exists for compositions consisting of more than 65% Ag. Our calculations used LSDA, ultrasoft pseudopotentials [15], and the plane wave basis set as implemented in the Vienna *ab initio* simulation package [16]. Ultrasoft pseudopotentials allowed treatment of localized transition metal  $d$  states using a manageable energy cutoff  $E_{\text{cut}} = 17.4 \text{ Ry}$  for the plane wave basis set. Because of the metallic character of the studied system, special attention was paid to Brillouin zone integrations. Standard equivalent  $k$  point schemes were used in calculating formation enthalpies of ordered surface structures, which ensure rapid convergence of energy differences due to the cancellation of systematic numerical errors. A finite-temperature Fermi-Dirac distribution, with  $T = 315 \text{ K}$

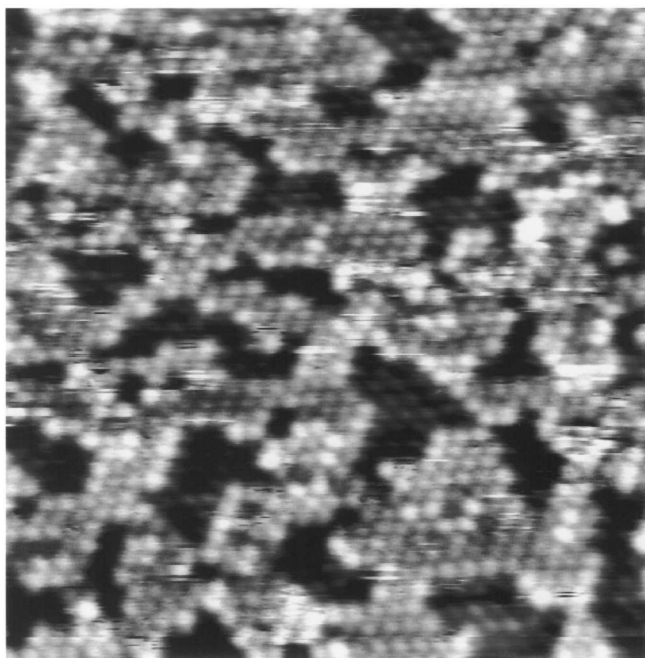


FIG. 2. Atomically resolved image ( $I_t = 50$  nA,  $V_s = -0.02$  V) of  $\text{Co}_{0.6}\text{Ag}_{0.4}$  alloy phase on Ru(0001). Ag atoms are darker; Co atoms are light colored. The image shows that Ag droplets are tens of atoms in size. Also, Co atoms that border Ag droplets are highly strained.

and hexagonal  $12 \times 12$  surface  $k$  point meshes or better, ensured convergence of the calculated formation enthalpies to within a few meV per surface atom. The surface alloy was modeled by a slab of six Ru layers with the seventh Co-Ag alloy layer on top. The three bottom layers of the Ru slab were held fixed at the calculated equilibrium geometry of bulk Ru (lattice parameter  $a_0 = 2.67$  Å and  $c/a = 1.58$  Å [17]). We considered a set of approximately 40  $\text{Co}_{1-c}\text{Ag}_c/\text{Ru}(0001)$  ordered surface structures. Most of the structures studied could be represented as periodic arrangements of  $(\text{Co})_m(\text{Ag})_n$  stripes along one of the two high-symmetry directions, [100] or [010] [Fig. 3(b)]. The set of structures also included simple periodic structures such as  $2 \times 1$ ,  $\sqrt{3} \times \sqrt{3}$ ,  $2 \times 2$ , etc., and two hexagonally ordered droplet phases ( $4 \times 4$   $\text{Co}_9\text{Ag}_7$  and  $3\sqrt{3} \times 3\sqrt{3}$   $\text{Co}_{20}\text{Ag}_7$ ) [Fig. 3(c)]. Details of our calculations will be discussed in a separate publication.

The energetic stability of a surface alloy structure is governed by its energy relative to other competing phases. We reference all energies relative to a state in which Co and Ag form phase-separated *pseudomorphic* patches on Ru(0001) [Fig. 3(a)], i.e., the formation energy of a surface alloy in structure  $\sigma$  is defined as

$$\Delta H(\sigma) = E(\sigma) - (1 - c)E_{\text{PSM}}(\text{Co/Ru}) - cE_{\text{PSM}}(\text{Ag/Ru}), \quad (1)$$

where  $E_{\text{PSM}}$  is the total energy per surface atom for a pseudomorphically strained layer, and  $c$  is the alloy composition. We find that all structures with many nearest-

neighbor Co-Ag bonds (e.g.,  $2 \times 1$ ,  $\sqrt{3} \times \sqrt{3}$ ,  $2 \times 2$ ) have strong positive formation energies, indicating that there is a large energetic cost associated with Co-Ag bonds, consistent with the immiscibility of bulk Co and Ag mentioned above. On the other hand, energies of sufficiently long-period striped phases are found to possess negative formation energies and change quite slowly for large periods  $\Lambda$ , as seen from the inset of Fig. 4 which shows the calculated formation energies of  $(\text{Co})_n(\text{Ag})_n$  stripes along [100]. Energetics of such systems in the continuum limit of elasticity theory have been studied by Ng and Vanderbilt [19], who found that simple periodic striped phases are favored near the 50-50 composition ratio, while hexagonally ordered patterns of droplets have lower energy below  $c = 0.29$ . Figure 4 shows  $\Delta H$  for the lowest energy striped phases at a few compositions (black circles), as well as the formation energies of  $4 \times 4$   $\text{Co}_9\text{Ag}_7$  and  $3\sqrt{3} \times 3\sqrt{3}$   $\text{Co}_{20}\text{Ag}_7$  hexagonal droplet phases (gray circles). We see that, in qualitative agreement with Ref. [19], periodic stripes are favored near  $c = 0.5$ , while the  $3\sqrt{3} \times 3\sqrt{3}$  droplet structure has a lower energy for  $c = 0.26$ .

To explain why alloy phases are not observed experimentally for all Ag compositions, we have calculated  $\Delta H$  for a  $(16 \times \sqrt{3})$  unit cell dislocation structure of Ag on Ru. As indicated by the filled square at  $c = 1$  in Fig. 4, we find that the introduction of dislocations lowers the energy of a Ag monolayer film by 39 meV per Ag atom [20]. The composition of the alloy phase at  $T = 0$  K can then be found by using the standard Gibbs construction, as shown by the common tangent tie line in Fig. 4. Because of the large decrease of energy in pure Ag films at  $T = 0$  K, Ag-rich striped alloy phases can find a state of lower energy by decomposing into the phases at the ends of the tie line, i.e., a  $\text{Co}_{0.35}\text{Ag}_{0.65}$  alloy and the dislocated Ag monolayer.

Our experimental results are qualitatively consistent with the calculated phase diagram in that we find coexistence of two phases. However, the theory predicts a *stripe* phase above Ag concentrations of 0.33, while experimentally we observe what appears to be a *droplet* phase at Ag concentrations of 0.4. In addition, the calculated Ag concentration of the coexisting alloy phase at  $T = 0$  K is slightly higher than the experimentally measured value

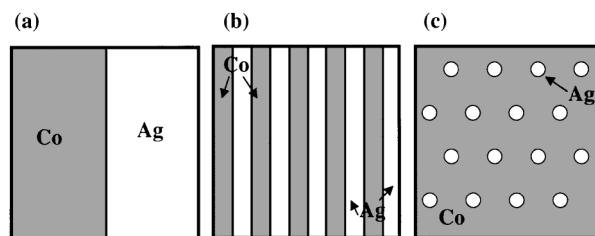


FIG. 3. Schematic representations of calculated configurations of Co-Ag: (a) reference state consisting of pseudomorphic phase-separated Co and Ag patches; (b)  $(\text{Co})_m/(\text{Ag})_m$  stripes along [100] or [010]; (c) hexagonally ordered droplet phases of Ag droplets in Co film.

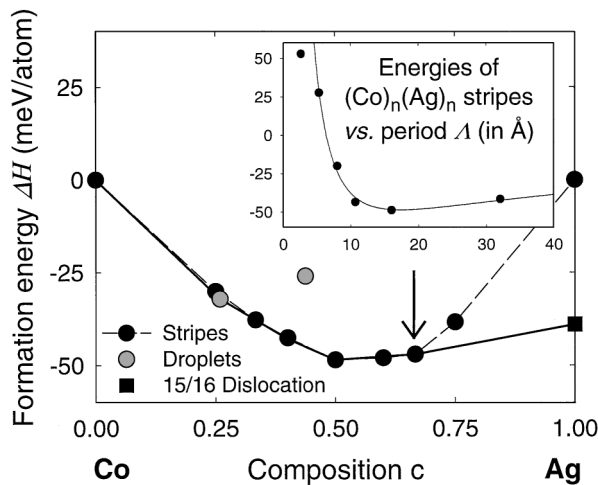


FIG. 4. Calculated formation enthalpies at  $T = 0$  K of Co-Ag stripes (black circles), droplets (gray circles), and 15/16 Ag dislocation on Ru(0001) (black square). The arrow points to the calculated composition for the onset of phase segregation. The solid line represents  $T = 0$  ground states. The inset shows formation energies of (100) stripe phases at  $c = 0.5$ . These properties of  $\Delta H$  indicated that the energetics of pseudomorphic  $\text{Co}_{1-c}\text{Ag}_c$  on Ru(0001) could be described by the model developed by Marchenko [18]. In particular, the solid line in the inset of Fig. 4 represents a fit to the calculated values of  $\Delta H$  using the expression [17,18]  $\Delta H = [I_c - I_E \log(\Lambda/a_{\text{Ru}})]/\Lambda$ , where  $I_E > 0$ ,  $I_c > 0$ , and  $\Lambda$  is periodicity.

at  $T = 800$  K. To explain the discrepancies we note that, when comparing the  $T = 0$  K calculations shown in Fig. 4 with the experimentally observed structures between 300 and 800 K, one has to take into account effects due to configurational and vibrational entropies. Qualitatively, these effects will modify the film structure in two ways. First, the long-range ordered droplet and stripe alloy phases will disorder above an order-disorder transition temperature,  $T_c$ . Above  $T_c$ , it is not meaningful to ask whether an alloy phase (such as the one shown in Fig. 2) represents droplets or stripes. Instead, one should consider it as a thermodynamically distinct disordered alloy phase with a degree of short-range order, i.e., a strong tendency among like atoms. Indeed, as seen from Fig. 2, patches of Ag can be interpreted as either elongated irregular droplets or short disconnected stripes. Second, vibrational and configurational contributions to the free energies of both coexisting phases can be substantial on the scale of Fig. 4, and could easily shift the equilibrium coexistence composition from the calculated value of  $c = 0.65$  to the experimentally measured value of  $c \approx 0.4$ . We also stress that this peculiar alloy phase is not a phase-separated state between Co and Ag, since the size of Ag clusters is limited and does not increase upon further annealing.

In summary, we find that thermodynamic phase diagrams of surface systems, which have available two or more distinct stress relief mechanisms, can have large coexistence regions due to the incompatibility of these mechanisms. In the case of CoAg/Ru(0001), there exists

a distinctive phase separation, which we attribute to the competitive stress relief mechanisms of mixing and dislocation formation. Our observations have some interesting implications. First, they clearly show that stress relief can result in surface phase diagrams that are different from the relatively simple progression of droplet and striped phases predicted by continuum theories such as that of Ng and Vanderbilt [19]. Second, it is striking that surface configurations as complicated as the one shown in Fig. 1(b) are actually close to the equilibrium structure of an alloyed surface. Since the competition in stress relief mechanisms that causes this type of structure will be a feature common to many surface alloys, the understanding of the phase separation that we observe contributes to the ability to control the nanoscale structure of surface alloys.

This work was supported by the Office of Basic Energy Sciences of the U.S. DOE, Division of Materials Sciences under Contract No. DE-AC04-94AL85000.

- [1] Peter Haasen, *Physical Metallurgy* (Cambridge University Press, Cambridge, UK, 1996), 3rd ed., p. 142.
- [2] R. Q. Hwang, J. C. Hamilton, J. L. Stevens, and S. M. Foiles, *Phys. Rev. Lett.* **75**, 4242 (1995).
- [3] C. Günther, J. Vrijmoeth, R. Q. Hwang, and R. J. Behm, *Phys. Rev. Lett.* **74**, 754 (1995).
- [4] J. Tersoff, *Phys. Rev. Lett.* **74**, 434 (1995).
- [5] L. Pleth Nielsen *et al.*, *Phys. Rev. Lett.* **71**, 754 (1993).
- [6] C. Nagl *et al.*, *Surf. Sci.* **321**, 237 (1994).
- [7] J. L. Stevens and R. Q. Hwang, *Phys. Rev. Lett.* **74**, 2078 (1995).
- [8] R. Q. Hwang *et al.*, *J. Vac. Sci. Technol. A* **10**, 1970 (1992).
- [9] J. W. Niemanstverdriet *et al.*, *J. Vac. Sci. Technol. A* **5**, 875 (1987).
- [10] C. Liu and S. M. Bader, *J. Magn. Magn. Mater.* **119**, 81 (1993).
- [11] These structures are not identical because the Ag chemical potential is different for the two systems.
- [12] *Binary Alloy Phase Diagrams*, edited by T. B. Massalski (ASM, Metals Park, OH, 1990), 2nd ed.
- [13] H. Roder, R. Schuster, H. Brune, and K. Kern, *Phys. Rev. Lett.* **71**, 2086 (1993).
- [14] O. L. Alerhand, D. Vanderbilt, R. D. Meade, and J. D. Joannopoulos, *Phys. Rev. Lett.* **61**, 1973 (1988).
- [15] D. Vanderbilt, *Phys. Rev. B* **41**, 7892 (1990).
- [16] G. Kresse and J. Hafner, *Phys. Rev. B* **47**, 558 (1993); *ibid.* **49**, 14251 (1994); G. Kresse and J. Furthmüller, *Comput. Mater. Sci.* **6**, 15 (1996); G. Kresse and J. Furthmüller, *Phys. Rev. B* **54**, 11169 (1996).
- [17] The experimentally measured value of the bulk Ru lattice parameter is 2.71 Å; LSDA values for lattice parameters are consistently smaller than those that are measured.
- [18] V. I. Marchenko, *Sov. Phys. JETP Lett.* **55**, 73 (1992).
- [19] K. O. Ng and D. Vanderbilt, *Phys. Rev. B* **52**, 2177 (1995).
- [20] Formation energy of a 15/16 dislocation per Ag atom was defined as  $H = \{E_{\text{DISL}}(16 \times \sqrt{3}) - 30E_{\text{PSM}}(\text{Ag/Ru}) - 2E_{\text{SURF}}(\text{Ru})\}/32$ , where  $E_{\text{DISL}}(16 \times \sqrt{3})$  is the total energy of a slab with a  $(16 \times \sqrt{3})$  unit cell Ag dislocation and  $E_{\text{SURF}}(\text{Ru})$  is the total energy of a  $1 \times 1$  Ru slab.